Available online at www.synsint.com

Synthesis and Sintering

ISSN 2564-0186 (Print), **ISSN** 2564-0194 (Online)

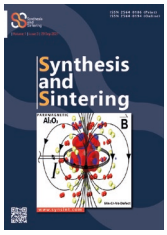

Research article

Wear behavior of self-propagating high-temperature synthesized Cu-TiO_2 nanocomposites

Hossein Aghajani [a,*], Mohammad Roostaei [b], Shaya Sharif Javaherian [b], Arvin Taghizadeh Tabrizi [a], Ali Abdoli Silabi [c], Navid Farzam Mehr [d]

[a] *School of Metallurgy and Materials Engineering, Iran University of Science & Technology, Narmak, Tehran, Iran*
[b] *Materials Engineering Department, University of Tabriz, Tabriz, Iran*
[c] *Iran Small Industries and Industrial Parks Organization (ISIPO), Tehran, Iran*
[d] *Institut fur Metallurgie, TU Clausthal, Clausthal-Zellerfeld, Germany*

ABSTRACT

In this paper, the copper-based nanocomposites with TiO_2 nanoparticles were synthesized by the self-propagating high-temperature synthesis (SHS) process. The effect of the different amounts of excess copper, in comparison with the stoichiometric ratio (CuO:Ti ratios of 1:1, 2:1, and 3:1), on the phase formation of achieved samples was studied. A thermodynamical study showed that increasing the excess copper powder reduces the adiabatic temperature, which helps the phase formation. The maximum Brinell hardness (89) was obtained for the sample with the CuO:Ti ratio of 1:1. Finally, the wear behavior of the synthesized nanocomposites was evaluated by the pin on disk test, and the variation of friction coefficient and lost weight were measured. The friction coefficient decreased by the formation of phases and distribution of titanium oxide particles during the SHS process in the presence of the stoichiometric ratio of CuO:Ti. Therefore, the wear behavior was improved. The lowest depth of wear trace was measured 0.68 where the ratio of CuO:Ti was 1:1.

KEYWORDS

Wear behavior
Synthesis
Thermodynamic
Cu-TiO_2

OPEN ACCESS

1. Introduction

Tribology which is defined as the science and technology of interacting surfaces in relative motions, has attracted increased attention from various fields in research [1, 2]. Wear resistance is one of the four tribological properties which affect the lifetime of many industrial parts and indicates their performance in diverse loading conditions [3, 4]. This feature of materials could be improved by two different methods. The first method is applying a protective surface coating [5, 6] and the second one is synthesizing wear-resistant composites [7, 8]. For approaching this aim adding diverse elements as reinforcement is one of the most common methods [9]. Studies have been conducted to investigate the effect of different elements like TiO_2 [7, 10], SiC [11], Al_2O_3 [12], etc.

It is worth mentioning that improving the wear resistance of the materials with weak surface properties including magnesium [13], aluminum [14], titanium [15], and copper [16] attracts more attention among researchers. Among these materials, copper-based nanocomposites have significant application in automobile, bio, energy-saving, steel making, and petrochemical industries due to their exclusive properties like high thermal and electrical conductivity, but as mentioned before, their application is restricted due to the low wear resistance of the surface [17, 18]. Therefore, the wear resistance of these materials must be improved to develop and broaden their application. Self-propagating high-temperature synthesis known as the SHS is one of the simplest, fastest, and economical methods of synthesizing different composites. SHS method is based on an

* Corresponding author. *E-mail address:* haghajani@iust.ac.ir (H. Aghajani)
Received 4 June 2021; Received in revised form 14 August 2021; Accepted 20 August 2021.

https://doi.org/10.53063/synsint.2021.1332

exothermic reaction between initial ingredients and it is taken place in an adiabatic container. Therefore, the generated heat by chemical reaction leads to the reaction in the whole sample. This method has a high potential for mass production of metallic nanocomposites [19, 20]. In our previous studies, the mechanical and electrical behavior of Cu-TiO_2 nanocomposite produced by mechanical alloying [21] and thermochemical routes [22] were studied. Also, the corrosion behavior of the SHS produced Cu-TiO_2 nanocomposites was studied [23]. In this paper, the wear behavior of the SHS-produced Cu-TiO_2 nanocomposites is studied by applying pin on disk wear test and the active wear mechanisms were determined by carrying out FE-SEM morphology studies. Also, the effect of the excess copper powder than the stoichiometric ratio was determined on wear behavior.

2. Experimental

2.1. Preparation for synthesis

Copper and titanium powders with high purity were used as initial components as raw materials for synthesizing the nanocomposite in this study. At the first stage, copper powders were oxidized at the furnace at 400 °C for 3 h by placing in a crucible made of alumina. The achieved oxidized copper powders were mixed with titanium powders with the stoichiometric ratio. To study the influence of excess copper powders on the wear resistance of obtained composite, excess amounts of copper with the ratio of 2 and 3 times higher than the stoichiometric ratio were combined to the stoichiometric mixture. The coding of the samples is presented in Table 1.

As the next step, and to activate the powders, powders were mixed in a ball mill for 5 minutes at 120 rpm and BP ratio of 6:1. 0.1 wt% poly-vinyl alcohol (PVA) solution (0.1 mole) and 0.7 wt% of zinc stearate ($C_{36}H_{70}O_4Zn$) were added to the mixed powder before the cold press to enhance the green strength. Cold pressing was applied under 150 MPa pressure in a mold with a diameter of 40 mm and 10 mm in height. Afterward, dehydration of the specimens was carried out for 1 hour in the oven at 130 °C. The SHS synthesis reactions were carried out according to our previous studies [23] and in a stainless-steel cylindrical vessel under an argon atmosphere with a pressure of 0.1 MPa. Ni-Cr electrode was used to initiate the combustion of samples and the propagation resulted from the combustion wave advanced through the other end of the samples. The electro-discharge machine (EDM-AH840-Mah Wire Cut-Isfahan-Iran) was used for the final cutting of the samples. Also, the calculation of Gibbs free energy was carried out through HSC V6.0 software.

2.2. Characterization

Before the SHS synthesis process initiation, a DTA test was carried out to determine the temperature of reaction with the DTA device model ETG-60AH with a heating rate of 10 degrees/min. The phase composition of specimens was determined by X-ray diffraction (XRD) with Cu Kα radiation source (1.5406 A) (Philips 1710 High-Resolution). After synthesis of nanocomposites, the microstructure of samples was revealed using Field Emission Scanning Electron Microscopy (FE-SEM-A Vega Tescan) and chemical analysis was carried out using X-ray energy dispersive spectroscopy (EDS) spectra for microstructure observation. The surface hardness test was applied by using Brinell hardness. Pin on disk wear test was applied to study the wear behavior of the samples based on ASTM G99. The loss weight of the samples after the wear test was measured. The tungsten carbide pin with a round surface (diameter: 5 mm) was chosen. The applied load was chosen as 10 N, distance 600 meters, and 0.06 m/s.

Table 1. Coding of SHS synthesized samples.

Code	CuO:Ti ratio
1CT	1:1
2CT	2:1
3CT	3:1

3. Results and discussion

XRD pattern of the oxidized copper is demonstrated in Fig. 1. It is obviously shown that the formation of both copper oxide phases, CuO and Cu_2O, was occurred, but it is exhibited that the height of the peaks belongs to the Cu_2O phase are more than peaks related to the CuO phase. Peaks at 36, 44, and 63 degrees indicate the formation of the Cu_2O phase, and peaks at 34, 42 degrees imply the formation of the CuO phase. Reactions 1 and 2 show the Gibbs free energy formation of these two phases. The XRD pattern (Fig. 1) shows that the peak intensity of the Cu_2O phase is more than the CuO phase. Despite the calculation of free Gibbs energy of Eqs. 1 and 2, where Cu_2O (of -119.5 kJ) has lower Gibbs free energy formation than CuO (of -94.22 kJ), the determined oxide phase is CuO which was obtained from the quantitative phase calculation carried out by MAUD software, CuO: 34%, Cu_2O: 29% and Cu: 37%. Also, peaks at 38, 62, and 74 degrees indicate the remained un-oxidized copper.

$$Cu(s) + 0.5\ O_2 \rightarrow CuO(s) \qquad \Delta G^0_{673} = -94.22\ kJ \tag{1}$$

$$2\ Cu(s) + 0.5\ O_2 \rightarrow Cu_2O(s) \qquad \Delta G^0_{673} = -119.5\ kJ \tag{2}$$

DTA diagram of mixed powders copper oxide and titanium is presented in Fig. 2. DTA test was carried out to determine the temperature of the reactions of Eq. 3 as below:

$$2CuO + Ti + xCu = (2+x)\ Cu + TiO_2 + Q \tag{3}$$

4 different peaks are determined in the DTA diagram of Fig. 2 which all of them are exothermic. The first peak is demonstrated at 250 °C which is related to the oxidation of copper powder and formation of Cu_2O phase and the second phase at 350 °C which indicates the oxidation of copper powder and formation of CuO phase. The third peak at 750 °C and the fourth peak at 850 °C in the DTA curve indicate the reaction of Cu_2O and CuO phases with titanium respectively. Therefore, it could be concluded that the temperature of reaction triggering is almost between 700 to 800 °C.

3.1. Synthesized nanocomposites

SHS process was carried out in the adiabatic container; therefore, by calculation of adiabatic temperature, the phase formation could be predicted. SHS method is based on exothermic reactions as is shown in Eq. 4.

$$A + B = C + Q \tag{4}$$

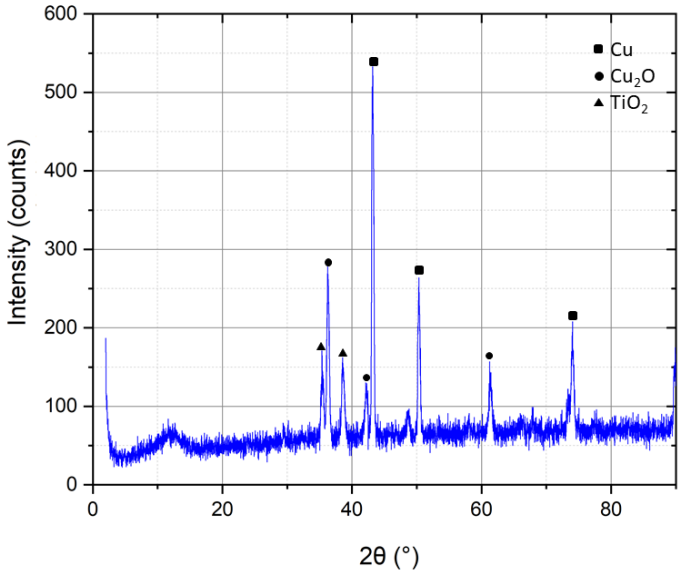

Fig. 1. XRD pattern of oxidized copper powder.

It is obvious that some heat, Q, was produced during the reaction between ingredients. Due to the adiabatic condition, the produced heat could be calculated by difference if the standard enthalpy of components and adiabatic temperature could be obtained. The diagram of the calculated adiabatic temperature versus excess copper powder in Eq. 3 is shown in Fig. 3. It is shown when the stoichiometric ratio of initial powders including copper oxide and titanium was used; the adiabatic temperature reaches 3600 °C. In other words, if the SHS process is carried out base on the stoichiometric ratios and without excess copper powder, the adiabatic temperature increases up to 3600 °C. Therefore, generated heat, Q, helps to continue the reaction and forwarding the combustion wave both vertical and horizontally and obtained a uniform microstructure. It is shown that by increasing the amount of excess copper powder, and due to the high thermal conductivity feature of copper powder, the adiabatic temperature is decreased. Therefore, less heat was available to continue the synthesis process and nonuniform nanocomposite could be achieved. The formation of the phases was studied in our previous study and the

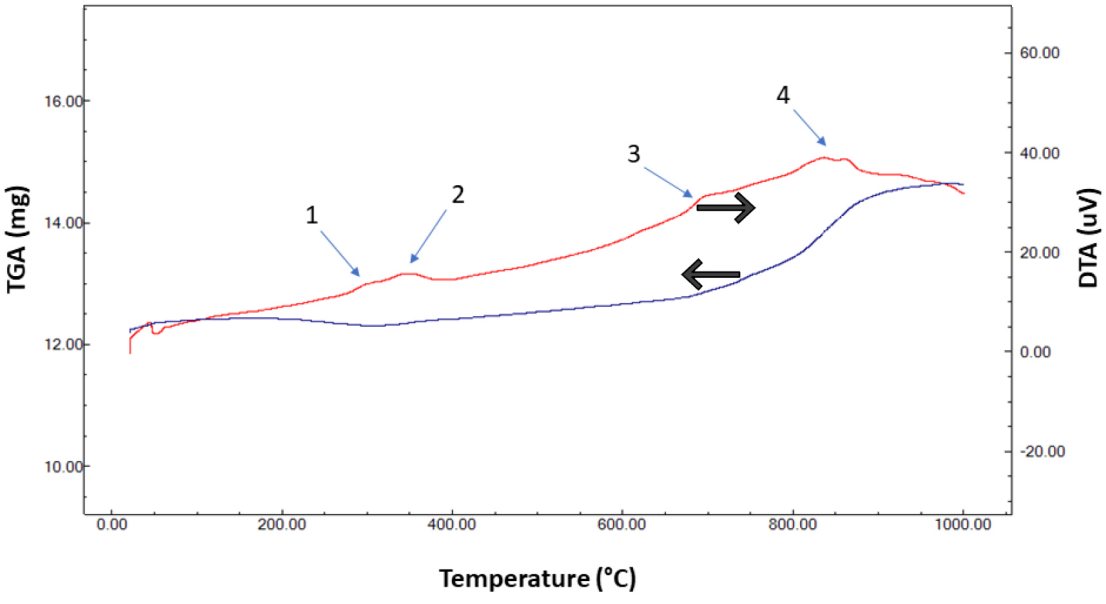

Figure 1 Fig. 2. DTA/TGA diagrams of mixed powders of copper oxide and titanium.

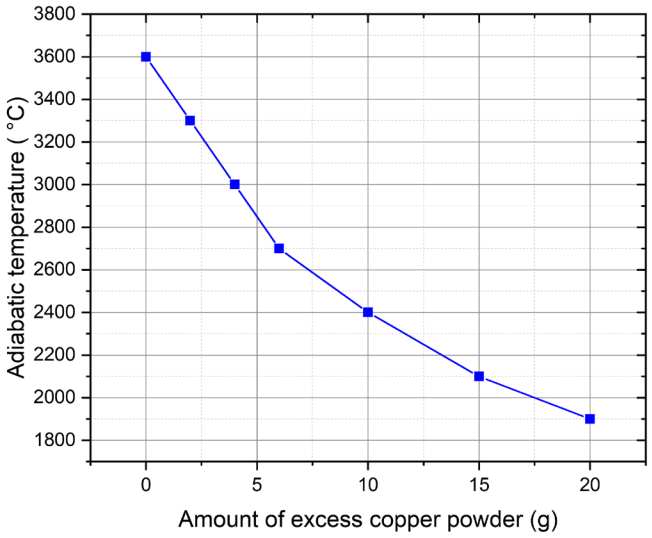

Fig. 3. Calculated adiabatic temperature versus the amount of excess copper powder.

formation of the phases including TiO_2, TiO, Cu_3Ti were detected [23]. Phase formation of the SHS produced copper titanium oxide nanocomposite and the effect of the excess copper were studied in our previous study. Uniformity of phase formation is essential to achieve homogeneous properties all over the sample. The nature intrinsic of the SHS process is to develop the combustion wave of the reaction zone. The forwarding of this reaction zone is dependent on the adiabatic temperature, powders amounts, and the soundness of the adiabatic container. For assuring the uniformity of the phase formation, XRD could be taken from different parts (surface and bottom areas) of the samples to study the phase formations. Considering the prepared synthesized sample, the XRD pattern of the surface and bottom section of the sample 1CT was shown in Fig. 4a and 4b. It is obviously seen that at the surface area of the sample, the unreacted copper oxide

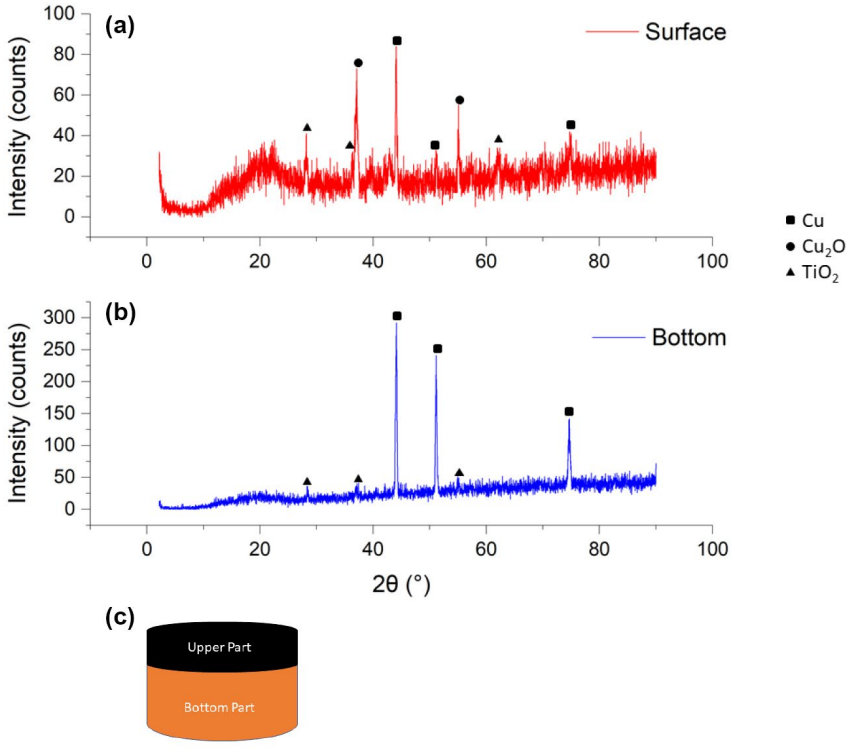

Fig. 4. XRD pattern of a, b) surface and bottom area of sample 1CT, and c) schematic of synthesized sample.

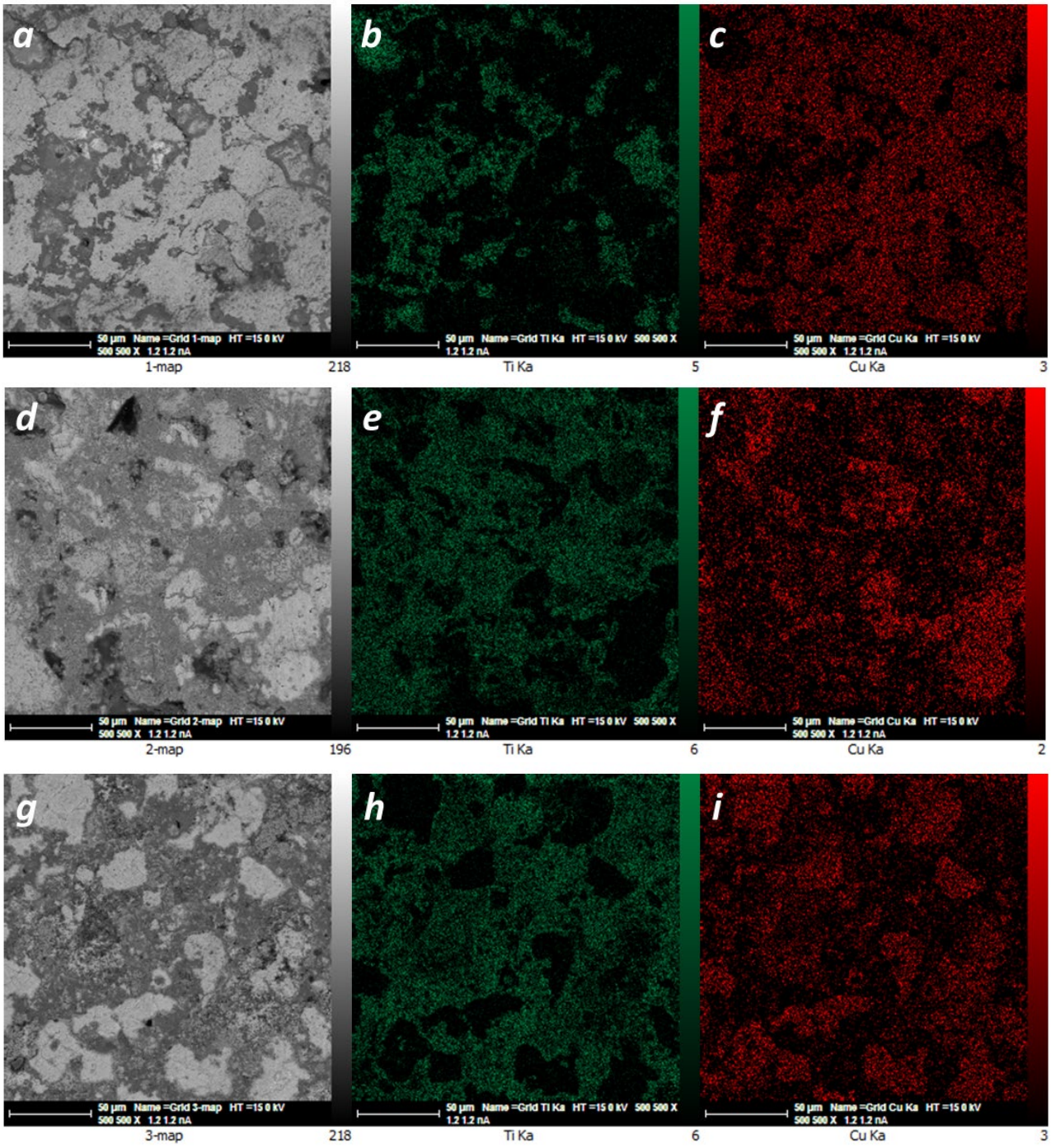

Fig. 5. FE-SEM and map analysis of titanium and copper powders distribution: a, b, c) sample 3CT, d, e, f) sample 2CT, and g, h, i) sample 1CT.

remained but at the bulk area, the combustion wave was forwarding successfully and the reaction of 3 occurred completely and copper and titanium oxide phases were obtained successfully.

The hardness of the obtained nanocomposites was evaluated by Brinell hardness and the effect of the excess copper was determined. It is shown that when the ratio of copper oxide to titanium powder equals the stoichiometric ratio, the measured microhardness value equals 89. By increasing the CuO:Ti ratio to 2:1 equals 72 and by increasing the ratio to 3:1, the hardness value decreased to 54. These values are lower than surface hardness which is reported in our previous study [24] for Cu-TiB_2 nanocomposite equals 105 HV. From the provided FE-SEM image and MAP diagrams of distribution of titanium and copper in Fig. 5 for synthesized samples, it could be declared that by increasing the titanium ratio in the initial mix powder, the distribution of formed titanium dioxide particle is reduced too and the microhardness is reduced respectively.

Obviously, there are many factors that influence the wear behavior of the diverse parts, including temperature, applied load, surface hardness,

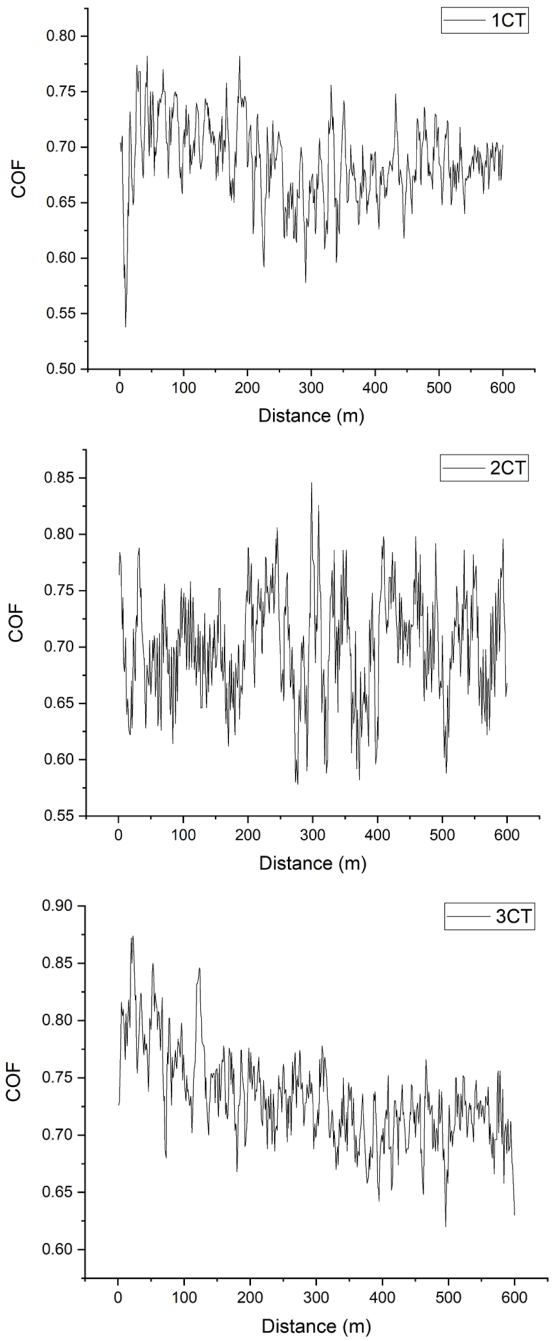

Fig. 6. Variation of friction coefficient of worn samples.

and surface parameters, etc., and the evaluation of the wear behavior could be performed during pin on disk wear test. Weight loss, variation of the friction coefficient, and variation of the depth of the wear trace are three important results that make it possible to compare the wear intensity. The wear test results are presented in Fig. 6 as the variation of friction coefficient to the wear distance which is known as the structure of the transferred layer. The low friction coefficient is one of the various aspects of better performance of parts that experience wears conditions. It is completely shown in Fig. 6, that the fluctuation of the friction coefficient is increased by increasing the amount of excess copper powder. The average of the COF measured 0.68±0.01, 0.70±0.01, and 073±0.01 in samples 1CT, 2CT, and 3CT respectively. Therefore, sample 1CT has better wear performance than other samples. In samples 3CT and 2CT, due to the presence of excess powder, the friction coefficient is higher than sample 1CT in all 600 m, but the difference at the initial distances is higher due to the soft intrinsic nature of copper powder leads this increase in the average of COF. By occurring the wear and formation of copper oxide due to the temperature increase at the interface of samples and wear a pin, this difference was reduced and as it is could be seen from Fig. 6, after

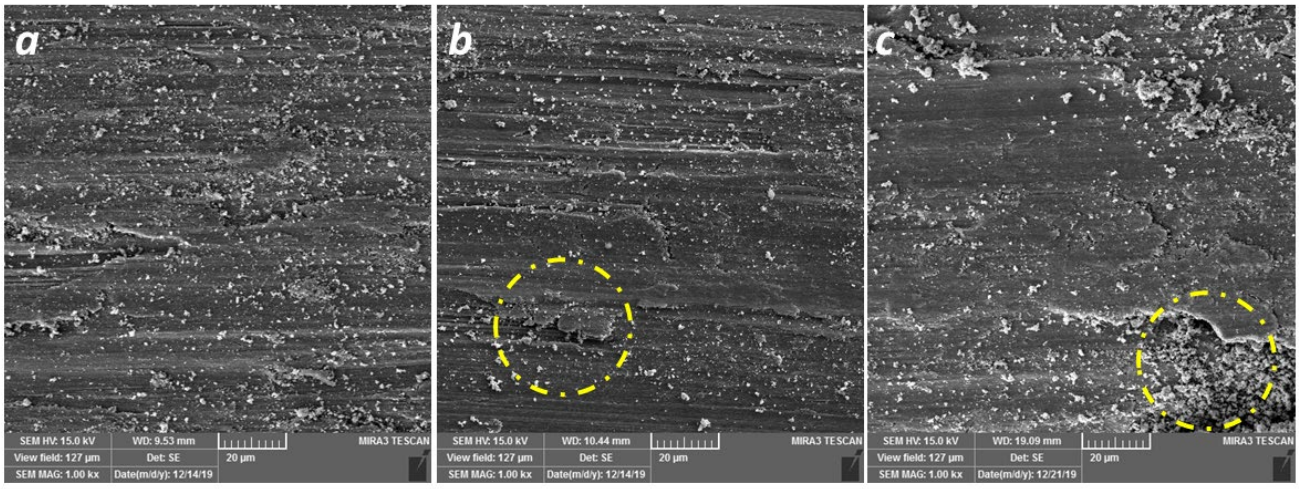

Fig. 7. FE-SEM images of wear trace of a) 1CT, b) 2CT, and c) 3CT.

450 m, the COF diagram overlaps with together more and just the range of the fluctuations are differ. Also, the lost weight of the samples is measured after the wear test as a symbol of the wear performance. The sample 1CT has minimum weight loss equals 0.04±0.01 g in comparison to other samples 2CT and 3CT where the lost weights equal 0.13±0.01 g and 0.19±0.01 g, respectively.

Diverse mechanisms have been proposed in the literature for severe wear where all of them are involved with plastic deformation, but little detail differences change how materials are removed and as a result change the active wear mechanism. Therefore, the wear traces of the samples were studied by FE-SEM to determine the wear mechanism. The FE-SEM images of the wear trace of samples are provided in Fig. 7. The delamination could be easily observed in the wear trace of samples 2CT and 3CT which are shown by yellow circles. This local delamination indicates the plastic deformation which is a sign of activation of the adhesive wear mechanism. The mechanism of removal of the materials and flakes-like sites is the sign of detachment of materials from the contact surface within the wear due to the adhesive wear mechanism. This is due to the lower distribution of the reinforcement in the copper matrix. On the other hand, FE-SEM image in Fig. 7a, no sign of the adhesive wear mechanism could be seen and only parallel lines could be detected which implies the abrasive wear. These parallel lines indicate the plastic flow at the asperity tips and followed by a detachment of wear particles. In these cases, adhesive forces are not the only factor for materials removal and other parameters like mechanical interaction between two contact surfaces must be considered [25].

4. Conclusions

Copper-TiO_2 nanocomposite synthesized by self-propagating high-temperature synthesis (SHS) process and the effect of the excess copper in comparison to stoichiometric ratio on the wear resistance of samples was studied. Results show that the addition of the excess copper reduces the adiabatic temperature and as result, the formation and distribution of the phases were not uniform. As a consequence, the wear behavior of the synthesized samples is weakened by increasing the excess copper powder and the optimized ratio of CuO:Ti is 1:1 for the synthesis of Cu-TiO_2 nanocomposite through the SHS method, and friction coefficient is measured equals 0.68 for this sample. The value of the friction coefficient is increased up to 0.7 and 0.73 for samples with CuO:Ti ratio of 2:1 and 3:1 respectively.

CRediT authorship contribution statement

Hossein Aghajani: Supervision, Conceptualization, Writing – original draft.
Mohammad Roostaei: Formal analyis, Investigation, Methodology.
Shaya Sharif Javaherian: Formal analyis, Investigation, Methodology.
Arvin Taghizadeh Tabrizi: Data curation, Writing – review & editing
Ali Abdoli Silabi: Methodology.
Navid Farzam Mehr: Formal analysis.

Data availability

The data underlying this article will be shared on reasonable request to the corresponding author.

Declaration of competing interest

The authors declare no competing interests.

Funding and acknowledgment

The authors express their gratitude to the University of Tabriz for their generous financial support and for providing the necessary instruments and equipment essential for the successful completion of this study.

References

[1] Z. Zeng, L. Wang, L. Chen, J. Zhang, The correlation between the hardness and tribological behaviour of electroplated chromium coatings sliding against ceramic and steel counterparts, Surf. Coat. Technol. 201 (2006) 2282–2288. https://doi.org/10.1016/j.surfcoat.2006.03.038.

[2] İ. Hacısalihoğlu, F. Yıldız, A. Çelik, Tribocorrosion behavior of plasma nitrided Hardox steels in NaCl solution, Tribol. Int. 120 (2018) 434–445. https://doi.org/10.1016/j.triboint.2018.01.023.
[3] J. Padgurskas, R. Kreivaitis, R. Rukuiža, V. Mihailov, V. Agafii, et al., Tribological properties of coatings obtained by electro-spark alloying C45 steel surfaces, Surf. Coat. Technol. 311 (2017) 90–97. https://doi.org/10.1016/j.surfcoat.2016.12.098.
[4] A.T. Tabrizi, H. Aghajani, F.F. Laleh, Tribological characterization of hybrid chromium nitride thin layer synthesized on titanium, Surf. Coat. Technol. 419 (2021) 127317. https://doi.org/10.1016/j.surfcoat.2021.127317.
[5] E. Marin, R. Offoiach, M. Regis, S. Fusi, A. Lanzutti, L. Fedrizzi, Diffusive thermal treatments combined with PVD coatings for tribological protection of titanium alloys, Mater. Des. 89 (2016) 314–322. https://doi.org/10.1016/j.matdes.2015.10.011.
[6] V.M.C.A. Oliveira, A.M. Vazquez, C. Aguiar, A. Robin, M.J.R. Barboza, Protective effect of plasma-assisted PVD deposited coatings on Ti-6Al-4V alloy in NaCl solutions, Mater. Des. 88 (2015) 1334–1341. https://doi.org/10.1016/j.matdes.2015.08.158.
[7] Q.Y. Hou, Microstructure and wear resistance of steel matrix composite coating reinforced by multiple ceramic particulates using SHS reaction of Al-TiO2-B2O3 system during plasma transferred arc overlay welding, Surf. Coat. Technol. 226 (2013) 113–122. https://doi.org/10.1016/j.surfcoat.2013.03.043.
[8] M. Ding, N. Sahebgharani, F. Musharavati, F. Jaber, E. Zalnezhad, G.H. Yoon, Synthesis and properties of HA/ZnO/CNT nanocomposite, Ceram. Int. 44 (2018) 7746–7753. https://doi.org/10.1016/j.ceramint.2018.01.203.
[9] S.A. Javadi, S.N. Hokmabadi, A. Taghizadeh Tabrizi, H. Aghajani, Corrosion behavior , microstructure and phase formation of ternary Ni–Ti–Si nano composite synthesised by SHS method, Powder Metall. 64 (2021) 341–350. https://doi.org/10.1080/00325899.2021.1906564.
[10] S.S. Javaherian, H. Aghajani, P. Mehdizadeh, Cu-TiO2 composite as fabricated by SHS method, Int. J. Self-Propag. High-Temp. Synth. 23 (2014) 47–54. https://doi.org/10.3103/S1061386214010051.
[11] A.R. Zurnachyan, S.L. Kharatyan, H.L. Khachatryan, A.G. Kirakosyan, Self-propagating high temperature synthesis of SiC-Cu and SiC-Al cermets: Role of chemical activation, Int. J. Refract. Met. Hard Mater. 29 (2011) 250–255. https://doi.org/10.1016/j.ijrmhm.2010.11.002.
[12] L. Li, Q. Bi, J. Yang, W. Liu, Q. Xue, Fabrication of bulk Al2O3 dispersed ultrafine-grained Cu matrix composite by self-propagating high-temperature synthesis casting route, Mater. Lett. 62 (2008) 2458–2460. https://doi.org/10.1016/j.matlet.2007.12.021.
[13] M.H. Fini, A. Amadeh, Improvement of wear and corrosion resistance of AZ91 magnesium alloy by applying Ni-SiC nanocomposite coating via pulse electrodeposition, Trans. Nonferrous Met. Soc. China. 23 (2013) 2914–2922. https://doi.org/10.1016/S1003-6326(13)62814-9.
[14] H. Pourbagheri, H. Aghajani, SHS-Produced Al–Ti–B Master Alloys: Performance in Commercial Al Alloy, Int. J. Self-Propag. High-Temp. Synth. 27 (2018) 245–254. https://doi.org/10.3103/S1061386218040052.
[15] T.S. Balasubramanian, M. Balakrishnan, V. Balasubramanian, M.A.M. Manickam, Influence of welding processes on microstructure, tensile and impact properties of Ti-6Al-4V alloy joints, Trans. Nonferrous Met. Soc. China. 21 (2011) 1253–1262. https://doi.org/10.1016/S1003-6326(11)60850-9.
[16] M. Ziemnicka-Sylwester, The Cu matrix cermets remarkably strengthened by TiB2 'in situ' synthesized via self-propagating high temperature synthesis, Mater. Des. 53 (2014) 758–765. https://doi.org/10.1016/j.matdes.2013.07.092.
[17] Y. Raghupathy, A. Kamboj, M.Y. Rekha, N.P. Narasimha Rao, C. Srivastava, Copper-graphene oxide composite coatings for corrosion protection of mild steel in 3.5% NaCl, Thin Solid Films. 636 (2017) 107–115. https://doi.org/10.1016/j.tsf.2017.05.042.
[18] S.A.N. Mehrabani, A.T. Tabrizi, H. Aghajani, H. Pourbagheri, Corrosion Behavior of SHS-Produced Cu–Ti–B Composites, Int. J. Self-Propag. High-Temp. Synth. 29 (2020) 167–172. https://doi.org/10.3103/S1061386220030061.
[19] V.V. Kurbatkina, E.I. Patsera, E.A. Levashov, A.N. Timofeev, Self-propagating high-temperature synthesis of single-phase binary tantalum-hafnium carbide (Ta,Hf)C and its consolidation by hot pressing and spark plasma sintering, Ceram. Int. 44 (2017) 4320–4329. https://doi.org/10.1016/j.ceramint.2017.12.024.
[20] Y. Liang, Q. Zhao, Z. Zhang, Z. Lin, L. Ren, Fabrication of bionic composite material using self-propagating high-temperature synthesis in the Cu-Ti-B4C system during steel casting, J. Asian Ceram. Soc. 1 (2013) 339–345. https://doi.org/10.1016/j.jascer.2013.10.004.
[21] Y.A. Sorkhe, H. Aghajani, A. Taghizadeh Tabrizi, Mechanical alloying and sintering of nanostructured TiO2 reinforced copper composite and its characterization, Mater. Des. 58 (2014) 168–174. https://doi.org/10.1016/j.matdes.2014.01.040.
[22] Y.A. Sorkhe, H. Aghajani, A. Taghisadeh Tabrizi, Synthesis and characterisation of Cu–TiO2 nanocomposite produced by thermochemical process, Powder Metall. 59 (2016) 107–111. https://doi.org/10.1179/1743290115Y.0000000020.
[23] G.N. Azari, A.T. Tabrizi, H. Aghajani, Investigation on corrosion behavior of Cu-TiO2 nanocomposite synthesized by the use of SHS method, J. Mater. Res. Technol. 8 (2019) 2216–2222. https://doi.org/10.1016/j.jmrt.2019.01.025.
[24] H. Aghajani, S.A.N. Mehrabani, A.T. Tabrizi, F.H. Saddam, Corrosion and mechanical behavior evaluation of in situ synthesized Cu-TiB_2 nanocomposite, Synth. Sinter. 1 (2021) 121–126. https://doi.org/10.53063/synsint.2021.1228.
[25] A.T. Tabrizi, H. Aghajani, H. Saghafian, F.F. Laleh, Correction of Archard equation for wear behavior of modified pure titanium, Tribol. Int. 155 (2021) 106772. https://doi.org/10.1016/j.triboint.2020.106772.